

# An EEG-based Experiment on VR Sickness and Postural Instability While Walking in Virtual Environments

Carlos Alfredo Tirado Cortes \*  
iCinema Centre,  
University of New South  
Wales

Chin-Teng Lin †  
Australian AI Institute,  
GrapheneX-UTS  
Human-centric AI Centre,  
University of Technology,  
Sydney

Tien-Thong Nguyen Do ‡  
Australian AI Institute,  
GrapheneX-UTS  
Human-centric AI Centre,  
University of Technology,  
Sydney

Hsiang-Ting Chen §  
School of Computer and  
Mathematical Sciences,  
University of Adelaide

## ABSTRACT

Previous studies showed that natural walking reduces the susceptibility to VR sickness. However, many users still experience VR sickness when wearing VR headsets that allow free walking in room-scale spaces. This paper studies VR sickness and postural instability while the user walks in an immersive virtual environment using an electroencephalogram (EEG) headset and a full-body motion capture system. The experiment induced VR sickness by gradually increasing the translation gain beyond the user's detection threshold. A between-group comparison between participants with and without VR sickness symptoms found some significant differences in postural stability but found none on gait patterns during the walking. In the EEG analysis, the group with VR sickness showed a reduction of alpha power, a phenomenon previously linked to a higher workload and efforts to maintain postural control. In contrast, the group without VR sickness exhibited brain activities linked to fine cognitive-motor control. The EEG result provides new insights into the postural instability theory: participants with VR sickness could maintain their postural stability at the cost of a higher cognitive workload. Our result also indicates that the analysis of lower-frequency power could complement behavioural data for continuous VR sickness detection in both stationary and mobile VR setups.

## Index Terms:

Human-centered computing—Human computer interaction (HCI)—HCI design and evaluation methods—User studies; Human-centered computing—Human computer interaction (HCI)—Interaction paradigms—Virtual reality

## 1 INTRODUCTION

Virtual Reality (VR) has become a mainstream product in the past few years. A recent report [3] found that six million VR headsets were sold worldwide in 2021 and evaluated the VR market size at 4.8 billion dollars. Despite the rapid growth of the VR market, VR sickness has long been considered a major issue that prevents the wider acceptance of VR technology. VR sickness shares similar symptoms to those of motion sickness. However, VR sickness presents stronger disorientation symptoms than other common symptoms such as headache, nausea, vomiting, and drowsiness [39, 75]. In 2016, a review article [62] reported that between 30% to 80% of head-mounted display (HMD) users experienced some VR sickness symptoms.

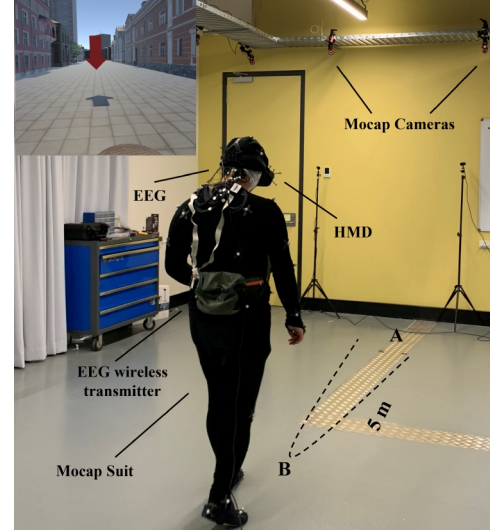


Figure 1: The experiment space and the motion capture system. The participant wore a motion capture suit, a 64-channel EEG headset, and a VR headset. The participant performs a VR walking task while physically walking between points A and B in each trial. Top-left corner shows the participant's view in VR.

The introduction of room-scale tracking to consumer VR headsets is a significant milestone in the fight against VR sickness. According to the sensory conflict theory, the mismatch between sensory inputs, e.g., visual and vestibular systems during passive movement, is the main source of VR sickness [39, 62]. Room-scale tracking allows users to navigate and interact with the virtual environment with natural walking, which reduces the sensory conflicts and the VR sickness symptoms [51]. However, even in a well-controlled lab environment, research studies still reported the occurrence of VR sickness symptoms despite using headsets and applications that allow natural walking [16, 37]. Indeed, recent studies found that VR sickness is still a prevalent human factor issue in modern consumer VR headsets [86], and around 5% of users had experienced severe VR symptoms [74]. Understanding the effect of VR sickness and its underlying cognitive and neural mechanisms is imperative to bring a comfortable VR experience for more users.

The VR community has accumulated a large volume of research on VR sickness [30, 66, 82]. The vast majority of these work used a stationary experiment setup [66] to study VR sickness. A common protocol is to keep the participant in the sitting posture and watch 360° videos or 2D abstract scenes with strong optical flows (Table 4 in [66]). Some works conducted EEG-based studies to understand the brain dynamics related to VR sickness (Table 3). These works further required participants to minimize head movements and stay in a stationary sitting posture to avoid introducing noise into the

\*e-mail: c.tirado@unsw.edu.au

†e-mail: Chin-Teng.Lin@uts.edu.au

‡e-mail: nguyenthiethong.do@uts.edu.au

§e-mail: tim.chen@adelaide.edu.au

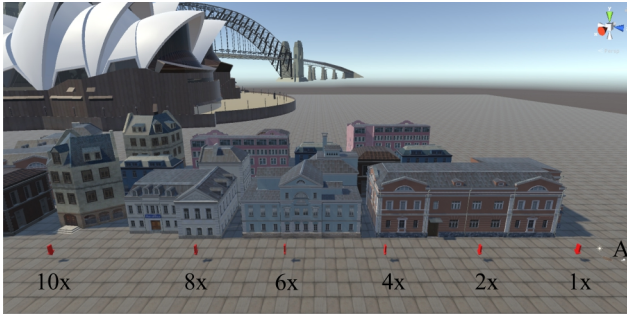


Figure 2: The side view of the virtual city. The red arrows indicate the mid-point of the virtual walking, where the participant turns and walks back to the starting point. Each red arrow corresponds to different levels of translation gain.

EEG signals. As most modern VR headsets allow users to navigate the virtual environment with natural walking, there is a knowledge gap about VR sickness in a mobile VR setup.

This paper aims to understand how VR sickness affects the user in a mobile VR setup using EEG and full-body motion capture. Our experiment follows the protocol in a previous work [81], which induces VR sickness by gradually increasing the level of translation gain (TG), i.e., the scale of mapping between the user's motions in the virtual world and those in the physical world [76, 83]. As the TG level increases beyond the detection threshold [77, 79], the perceived disparity between the virtual and physical worlds would also increase. The paper [81] showed that the increased disparity would eventually cause postural instability and VR sickness.

In this paper we hypothesise that, rather than sensory conflicts, postural instability is a higher driver for VR sickness in mobile VR setups. The hypothesis is based on two previous findings: first, previous studies suggested that mobile VR decreases sensory conflicts [28, 52]. Second, previous studies suggested that wearing a VR headset in a standing position would produce postural instability [23, 65], and the differences in biomechanics between locomotion in the virtual and the real world would also lead to the loss of body control [28, 65]. We believe that the diminished sensory conflict cues and increased efforts in postural control in mobile VR setups make the postural instability theory [64] intriguing in the mobile VR context. We hope this EEG-based study will provide new insights and data to this debate.

Our experiment used biomechanical measurement (full-body motion capture), neurological measurement (64-channel EEG), and self-reported questionnaires (Figure 1). During the experiment, the participant was instructed to walk toward a destination marked by a red arrow and back to the starting point inside a virtual city with increasing TG levels, including 1x, 2x, 4x, 6x, 8x, 10x (Figure 2). Based on the questionnaire responses, participants were divided into two groups: the VRS group, i.e., the participants who experienced strong VR sickness symptoms, and the NoVRS group, i.e., the participants with little to no VR sickness symptoms. A between-group analysis was conducted to understand the relationship between VR sickness and the users' biomechanics and neurological characteristics in the mobile VR setup. Note that the experiment design does not randomize the TG level because the experiment was not intended to evaluate the effect of TG levels on VR sickness.

## Contributions

- To the best of our knowledge, this paper presents the first EEG-based study investigating VR sickness in a mobile VR setup, i.e., the user navigates a virtual environment with natural walking while wearing a VR headset.

- The experiment recorded both EEG and full-body motion capture data, our preliminary results can contribute new evidence to the ongoing debate about the validity of postural instability theory and inspire future work in this area.

- The related work section presents a detailed literature review of EEG-based experiments for VR sickness. The review summarises the experiment protocols and apparatus used in previous works and the observed brain dynamic changes associated with VR sickness.

## 2 RELATED WORK

The VR community has accumulated a large volume of research studying VR sickness, and we would like to refer readers to several excellent survey articles [6, 62, 66] for complete reviews. This related work section complements these survey articles and focuses on works that used EEG to measure VR sickness and postural instability.

### 2.1 EEG and VR sickness

Recent advances in BCI hardware and signal processing algorithms have enabled novel BCI applications and paradigms [1]. Passive BCI [88], which continuously monitors the users' cognitive states, has been proven particularly valuable in many human-computer interaction scenarios. For example, Peck et al. [58] used BCI to evaluate visual interfaces. Frey et al. [18] proposed an EEG-based framework that estimated the user's mental workload and attention from EEG signals to evaluate user experience. Yuksel et al. [87] developed a BCI-based learning system that adaptively provides music learning tasks with different difficulty levels to enhance the user's learning efficiency.

There is a growing body of research on monitoring motion sickness and VR sickness from the VR community using the EEG-based passive BCI approach. (Table 3). One of the major benefits of using passive BCI for monitoring VR sickness is its capability to measure the sickness level continuously. Most VR works use questionnaires, such as Simulator Sickness Questionnaire (SSQ) [31], Virtual Reality Sickness Questionnaire (VRSQ) [32], or Cybersickness Questionnaire (CSQ) [78], to measure the VR sickness symptoms during VR uses. Despite its many advantages [22], the natural constraint of questionnaires is that they can only be conducted when the user is not actively performing the task. Some previous works used an additional joystick [8, 9, 36] or a physical dial [48] to allow frequent reports of the level of sickness. However, these additional input modalities still introduce different levels of distraction. In contrast, the passive BCI approach provides continuous measurements and does not incur additional workload or distract users from their current tasks.

Table 3 lists research works that investigated VR sickness using the passive BCI approach. Because these works used a wide range of experiment protocols to induce VR sickness, we sorted this list of works accordingly to their experiment designs and apparatus. The most common protocol for inducing VR sickness is to expose the participants to video content with strong motions, such as virtual navigation [34, 40, 49, 50, 56] or virtual flythrough [29, 36, 41, 53, 85]. The virtual navigation videos mostly involved the urban virtual environment with streets, roads, and sometimes obstacles. The virtual flythrough videos show a wider range of content, from flying to spacewalking, which exhibit stronger roll and pitch motions. The participants were mostly instructed to stay in a stationary sitting posture and passively watched the video content throughout the experiment session. Keeping the participant stationary is common in EEG-based experiments because it will reduce the potential noise in the EEG signals due to body movements. The participants' passive watching of identical video contents also ensures they perceive similar visual stimuli, allowing more precise time-locked EEG analysis if required.

Several works extend the 2D video setup by incorporating a motion platform to provide visual and vestibular stimuli. A series of works [8, 42, 43] used an experimental setup that included a CAVE and a vehicle mounted on a 6-degree-of-freedom motion platform. During the experiment, the participants behaved as a passenger in the vehicle as the vehicle automatically drove through a winding tunnel. The same group later updated the protocol to include an additional driver actively driving the vehicle through the tunnel [25]. Recent work from Recenti et al. [63] simulates seasickness with a virtual environment of a small boat floating on the sea. The participants wore an HMD while standing on a motion platform that generated synchronized vibrations to the virtual wave.

As shown in Table 3, most previous works reported the fluctuations of low-frequency band power when the participant experienced VR sickness. However, some changes in the power spectrum and the locations of brain activities are contradictory among these works. For example, among works that induced VR sickness with videos on a 2D display, some works [29, 34, 41] reported a low-frequency power increase while others [49, 56] reported a power decrease. Considering the difference in experiment protocols, hardware (displays and EEG headsets), and EEG signal processing protocols, such inconsistency in frequency band power is unfortunately not uncommon in BCI research. As a result, recent work [85] explores the reactive BCI paradigm [88], which uses more reliable brain dynamic features (e.g., event-related potentials). However, such brain features require strict time-locked events, which significantly limit the design of VR scenarios. There are also works [40, 43] focusing on using a machine learning approach to train classifiers that can detect or predict the onset of the VR sickness while putting less emphasis on the changes of spectrum powers and the underlying brain dynamics.

Complementing these previous works, our work investigates EEG changes of VR sickness while the participant actively navigates the virtual environment with natural walking. As most modern VR headsets allow users to move freely in the physical space, we believe our work represents a meaningful contribution to the understanding of VR sickness. Note that the mobile VR setup inevitably introduces additional noise into the EEG signals [46] and requires additional post-processing of the EEG signals. We describe our EEG data processing pipeline in detail in Section 4.2.

## 2.2 Postural Instability

We used an experimental protocol [81] inspired by the research works on redirected walking, originally developed for users to explore large virtual environments inside a limited physical space [52, 77, 79]. These works carefully control the amplification below the user's detection threshold [19, 37, 76]. In contrast, we intentionally increase the translation gain so that the users can perceive the disparity. The protocol hypothesizes that the disparity of movements between the virtual and physical worlds would require the user to adjust their gait strategies to maintain postural stability. As the disparity gradually increases in the experiment, the users would need to consistently change their posture to fight the postural instability. According to different studies on postural instability [74] as the users remain unstable, the level of VR sickness would also increase.

There is a significant amount of works and evidences both for and against the postural instability theory, and we would like to direct our readers to a recent review [55]. Here we would like to focus the review on works that use VR and BCI to measure and understand human balance control. The main applications of these research works are in the domain of fall prevention for elderly adults or performance enhancement in rehabilitation settings [84].

The seminal works from Slobounov et al. investigate brain functions and behaviour outcomes using experimental methods such as self-initiated postural sways [70, 71] and postural instability induced by rotating the virtual environment [72, 73]. These works agreed on theta power increases in the frontal areas during postural instability.

Chang et al. [5] induced postural instability with a virtual bus scenario on a motion platform to compare the brain activity of elderly adults with low and high fall-risk potential. The result suggested a strong correlation between postural-related cortical regions for the low fall-risk group. Peterson et al. [59] found that transient visual perturbations, i.e., a short roll of the virtual environment while the user is walking on a treadmill, could boost short-term motor learning, supported by the increased theta power and decreased alpha power in parietal and occipital regions and better balance performance. Many previous works also correlate the EEG signals with biomechanical measurements, such as the centre of pressure with force plate [73] or gait kinematics with motion tracking [59].

Building on the methodologies of these previous works, we contribute the knowledge of the brain dynamic related to posture and gait when the user experiences VR sickness in a mobile VR setup.

## 3 EXPERIMENT

### 3.1 Participants

Twenty-one healthy adults (17 males and four females) participated in the experiment. The mean age was 25.73, with a standard deviation of 3.6. All participants gave written informed consent and were compensated for their participation. All participants had a normal or corrected-to-normal vision. Among all participants, 13 had experience with 3D computer games, nine had experience in VR, and 15 had previous experience with motion sickness.

### 3.2 Physical Space and Virtual Environment

The physical space of the experimental environment was 3 meters by 5 meters (Figure 1). In each trial, the participant walked from point A to point B and back to point A. Points A were marked with black tape on the ground to ensure the participant stood at the proper initial position. The distance between A and B was 5 m.

The virtual size of the entire virtual scene was 100 m by 100 m. The virtual walking took place on a straight street 70 meters long and 5 meters wide. Figure 2 shows the side view of the road, and Figure 1 shows the participant's first-person perspective while performing the walking task. We marked both ends with a virtual utility hole and a virtual red arrow.

The virtual environment was developed using the Unity 3D game engine, version 2019. The virtual environment images were transmitted to the VR HMD via cable.

### 3.3 Apparatus

The user's full body motion was captured with the OptiTrack system with 12 Flex 13 cameras at the capture rate of 120 frames per second. We used the *Baseline + Toe marker* skeleton template with 41 tracked markers in the Motive:Body software for all participants. The HMD used in the experiment was the Oculus VR CV1, which has a 110-degree field-of-view resolution of 1080 x 1200 pixels per eye. The cable of the VR headset hung on a ceiling hook to avoid affecting the participants' movements. The OptiTrack Unity Plugin, which only supported Oculus VR CV1 at the time of the experiment, was used to synchronize the data between the motion capture system and the virtual environment.

The EEG data were recorded from 64 Ag/AgCl slim active sensors positioned according to the extended 10-20 electrode placement system. A portable and wireless LiveAmp system (Brain Products GmbH, Munich, Germany) was used to minimize the interference of natural walking in the virtual environment. The wireless LiveAmp receiver was on a waist bag, as seen in Figure 1. The EEG data were acquired at a sampling rate of 500 Hz. The channel locations were assigned based on standard location, distributed by the EEGLAB toolbox [11, 12]. Contact impedance was maintained below  $5k\Omega$  for the EEG recording.

### 3.4 Experiment Design

The experiment induces VR sickness by gradually increasing the level of translation gain. The experiment starts from TG level 1x, where the user's movements in the real world are directly mapped to the virtual environment without amplification. In each trial, the participant walks from the utility hole to the mid-point indicated by a red arrow, then back to the utility hole in the virtual city (Figure 1). The TG level increases every 5-trials (a *block*), in the order of 1x, 2x, 4x, 6x, 8x, 10x. The experiment consists of six blocks, each corresponding to one TG level, and there are 30 trials for each participant. The participant walks the same physical distance in the real world in each trial, regardless of the TG level. The TG level augments the virtual walking distance and thus the different mid-point locations, indicated by the red arrows (Figure 1).

An informal pilot test led to our decision of using 10x gain as the upper bound of the TG level. The VR engineer in our team, who has extensive experience in different redirected walking tests, considered TG levels larger than 10x impractical and too difficult for the participant to complete even one trial. Our implementation applied motion magnification to all axes, which is different from the traditional implementation [27], which amplifies the motion in the forward direction only. The decision was intended to ensure that participants were under constant motion magnification and postural instability throughout the experiment.

Participants were split into the *VRS* and *NoVRS* groups based on the SSQ after the experiment. The *VRS* group consists of participants who experienced severe VR sickness symptoms while interacting with the virtual environment. The *NoVRS* group consists of the participants that experience minor or null VR sickness symptoms during the experiment. Each group had two female participants.

Note that our experimental design does not randomize the order of TG levels as we do not intend to investigate the relationship between the TG level and the level of VR sickness. Instead, similar to previous EEG experiments that used multi-block designs [49, 53, 56], we compare the biomechanical and EEG data between *VRS* and *NoVRS* groups in each block to understand the effect of VR sickness at different experimental stages. We want our outcomes to be the preliminary results of one of the first experiments to address VR sickness on a mobile VR setup.

The supplemental video shows two trials with the TG levels of 1x and 2x. Please note that our participants did not agree to be recorded during the experiment. Thus the video is demonstrated by a researcher.

### 3.5 Procedure

Figure 3 shows the complete experiment procedure. The session started with a *pre-experiment questionnaire (PEQ)*. The PEQ inquired about the participants' familiarity with 3D and VR technologies and their subjective assessment of their susceptibility to different types of motion sickness. After completing the PEQ, the researcher helped the participant put on the motion capture suit and ensured the participant's full-body motion within the experiment area could be successfully captured and displayed in the software. After completing the motion capture setup, the researcher proceeded with the EEG headset setup. The researcher injected conductive gels into each of the 64 electrodes and ensured its impedance shown on the EEG capture software was below  $5k\Omega$ . The EEG signals of the closed-eye resting and eyes blinking were also visually inspected after the setup.

After the EEG and motion capture systems were ready, the participant performed the baseline walking trials (without wearing the VR headset). The participant was instructed to walk between the two ends of the walking area, i.e., from position A to B, then back to A in Figure 1. After the baseline walking, the researcher helped the participant put on the VR headset and adjusted the interpupillary distance. Wearing a VR headset would inevitably cause physical

contact with the electrodes. Thus, re-calibration and re-gel were usually required to correct the position and impedance of the EEG electrodes. The setup was completed at this point, and the setup process took around 40 to 50 minutes on average.

As stated in the experiment design section above, the main experiment consists of 6 blocks, each with 5 trials of one TG level. The TG level increases from 1x in the first block to 10x in the last block. In each trial, the participant walks toward a red arrow and back to the utility hole (Figure 2) in the virtual city. Once the participant reaches the utility hole, a virtual message notifies the completion of the trial. It then prompts the participant to report their level of sickness from 1 to 10, where ten corresponds to severe VR sickness symptoms.

## 4 MEASUREMENTS

### 4.1 Questionnaires

Besides the PEQ, this experiment uses two types of questionnaires. The first questionnaire is the **Between-Trial Questionnaire**. At the end of each trial, each participant reports, on a scale from 1 to 10, their feelings of dizziness, discomfort, nausea, fatigue, headache, and eyestrain. We chose these symptoms following previous studies [43, 83], which also used a sub-set of symptoms in trials to shorten the report time.

The second questionnaire is the **Post-Experiment Questionnaire**. Upon completing the VR session, we asked each participant for a full SSQ, followed by a semi-structured post-hoc interview session where the researchers engaged with the participant and recorded their subjective experience during the experiment.

### 4.2 EEG Data Processing

The following subsections describe our methodologies to process and analyze the EEG data of our experiment. Mobile VR with EEG experiments have well-established procedures to ensure that EEG data gets the highest signal-to-noise ratio. To ensure this, the following sub-sections briefly describe the same procedures as Do et al. [13]. The extensive work of these authors describes the methodologies of mobile experiments with VR and EEG.

Our work also follows the procedures from studies that describe how to remove gait-related artifacts [15, 44]. These procedures help minimize gait-related activity and do not affect any of the conclusions of this study. All the EEG data analysis steps were performed in EEGLAB [11, 12] version 14.1.2 in Matlab (Mathworks Inc., Natick, Massachusetts, USA). Figure 7 shows a summary of the EEG processing steps.

#### 4.2.1 EEG Pre-processing

The basis of the EEG pre-processing methods are previous EEG studies that use ambulatory VR setups [13, 45]. The EEG data was first down-sampled, applied a band-pass filter, and cleaned. The cleaning process includes using the *CleanLine* plug-in (v1.03), removing flat segments, and removing bad channels. Next, an independent component analysis (ICA) was used to extract the maxima independent source activation. The adaptive mixture independent component analysis (AMICA) [54] was used for this step. Finally, the eye components were removed. A more detailed description of the pre-processing step can be found in Appendix A.

#### 4.2.2 Data Grouping

For our analysis, including all the 64 channels of data was not useful because, in EEG channel-based studies, there will be redundant information since the individual EEG channel correlates with its neighbor channels. Thus, we picked up the representative channels which reflect the major brain regions in human brain experiments [21]. These are the midline-frontal region (Fz), central (Cz), parietal (Pz) and temporal (T8). Subsequently, based on the participant's

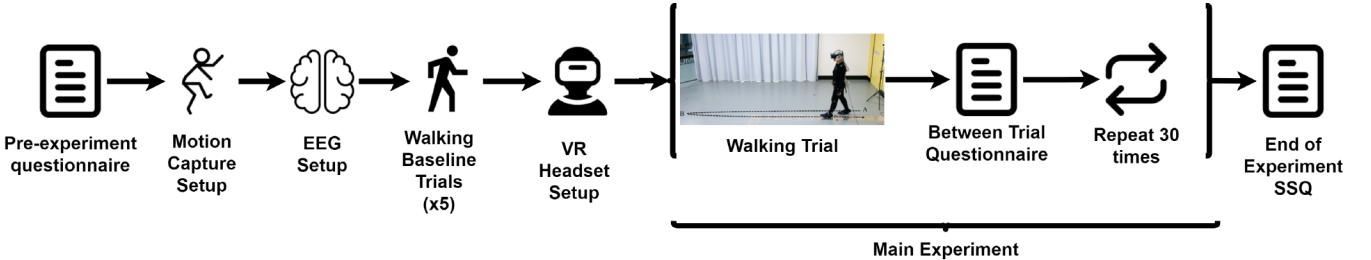


Figure 3: Flow of the experiment session.

SSQ responses, the data were divided into two groups: the *VRS* group and the *NoVRS* group.

#### 4.2.3 EEG Post-Processing

The walking EEG data segment was extracted from the continuous EEG data into 35 segments, each representing a trial. To calculate the epoch length, we decided to use the first three-quarters of a walking trial after the participant turned to start walking toward the red arrow. Because of the noise derived from the 180-degree turn, the study lost several data sets. Therefore, the first three-quarters were used to avoid any noise from the body turning. To calculate the exact time, we averaged the times of each trial of each condition from all the participants. The final epoch length was defined based on the shortest time interval of all the walking segments, which was 8 seconds.

For the noise removal, any values outside the  $\text{mean} \pm 3\text{std}$  were identified as noise values and were removed. During this process, we realized that the first trial of the experiment for all participants fell into this category. Further analysis revealed that most participants interrupted the trial to ask questions, adjust the headset, or do other things that caused noise in the EEG signals. This process also led to the data removal of two participants.

Then, the Event-Related Spectral Perturbation (ERSP) was used to transform the time series EEG data into the time-frequency domain (refer to [13]). In the ERSP time-frequency domain, the noise trials were removed if they were outside the  $\text{mean} \pm 3\text{std}$ . This method has demonstrated the feasibility of mobile EEG data analysis in previous studies [13]. Subsequently, the ERSP data recorded during the walking trials without a VR headset were used as a baseline. EEG analysis requires normalizing the data with an appropriate baseline that removes any individual artifacts introduced by the user's cognitive state before the study starts [10]. To deal with these artifacts and highlight the changes produced by VR sickness and postural instability in participants, the signals of the user walking without any of the cortical effects that the VR headset produces were selected as the baseline. Finally, the statistical test was performed to check the significant difference between blocks (concatenated all the participant data given their sickness group) and without VR headset using a permutation test ( $n=2000$  permutations) with false discovery rate correlation (FDR,  $\alpha=0.05$ ). The non-statistical difference values of the group ERSP data were removed, and the significant difference values were retained for the final visualization on the grand average of all participants, e.g., Figure 8, 6, and 9.

### 4.3 Biomechanical Measurements

#### 4.3.1 Center of Mass Calculation

The displacement between the CoM measured during the baseline walking trials without the VR headset and the CoM measured during virtual walking at different trials was calculated to analyze the change in CoM. The methodologies described by Lafond et al. [38] were used to calculate CoM. Because the speed of movement of the

CoM varied among the different trials for each participant, we followed the procedure by Adistambha et al. [2]. They used Dynamic Time Warping (from MATLAB's Dynamic Time Warping function) to align the different CoM signals.

#### 4.3.2 Gait Parameters

The gait parameters we calculated were step distance, cadence, and time to complete a trial. Step distance was calculated based on the motion of the markers on the participant's feet. The step information was extracted following the work by Hreljac and Marshall [24]. The function *findpeaks.m* from MATLAB, with the *MinPeakProminence* parameter set to 0.01 to remove all the noise peaks, was used to detect the upwards and downwards movements of the feet. These calculations helped calculate the number of steps a user used in each trial. Finally, we used each user's number of steps per minute to calculate cadence.

## 5 RESULTS

Excluding the experiment setup time, the main experiment took about 25 minutes per participant. Among the 21 participants, five participants were removed due to hardware malfunction or excessive noise in the EEG data. Out of the 16 remaining participants, three terminated earlier due to severe VR sickness completing 16, 20, and 22 trials and one completed 34 of the 35 trials.

The Shapiro-Wilk test was used for the behavioural measurements to test their normality. If the data followed a normal distribution, a Welch's t-test was used to compare the measurements between the two groups. Otherwise, a Kruskal-Wallis H-test was used for the comparison. For the EEG data, to avoid the Multiple Comparison Problem [47], we used the EEGLAB's permutation test ( $n=2000$ , FDR-correction) [17, 47] to identify the significant difference between the *VRS* group and the *NoVRS* group. We used the unbalanced version of the respective tests to test experiment blocks with an unbalanced number of trials.

### 5.1 Behavioral Results

#### 5.1.1 Post-Experiment SSQ

Kennedy et al. [31] and Stanney et al. [75] suggested a threshold of 18 on the total severity (TS) score as an indicator of a problematic level of sickness. The *VRS* group consisted of 8 participants with a TS score of 18 or higher. The *VRS* group had TS score of  $\mu = 39.4850$ ,  $\sigma = 17.378$ , Nausea score of  $\mu = 47.7$ ,  $\sigma = 19.7497$ , Occulomotor score of  $\mu = 41.69$ ,  $\sigma = 35.0886$  and Disorientation score of  $\mu = 107.88$ ,  $\sigma = 44.488$ . The *NoVRS* group consisted of 8 participants with a TS score of 18 or lower. The *NoVRS* group had TS score of  $\mu = 6.0225$ ,  $\sigma = 5.3411$ , Nausea score of  $\mu = 14.31$ ,  $\sigma = 11.4025$ , Occulomotor of  $\mu = 9.475$ ,  $\sigma = 13.2843$  and Disorientation score of  $\mu = 12.18$ ,  $\sigma = 15.6738$ .

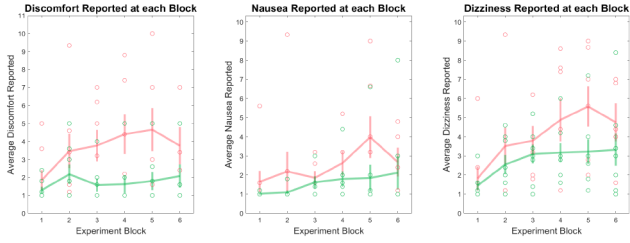


Figure 4: The discomfort, nausea and dizziness scores of the *NoVRS* group (green) and the *VRS* group (red). The bars represent the standard error. The dots represent the individual average of each user, in each experiment block.

Measure	B	Stat, p-val	$\mu$	$\sigma$
Disc.	3	$\chi^2(13) = 4.92, 0.02$	VRS 3.77 NoVRS 1.57	2.31 1.04
Disc.	4	$\chi^2(13) = 5.39, 0.02$	VRS 4.4 NoVRS 1.625	2.91 1.40
Disc.	5	$\chi^2(13) = 4.40, 0.03$	VRS 4.65 NoVRS 1.8	3.15 1.41
Nausea	5	$\chi^2(13) = 4.40, 0.03$	VRS 3.98 NoVRS 1.85	2.88 1.95

Table 1: Behavioral measurements with significant differences. Disc. stands for Discomfort. The second column is the block number. The third column shows the statistic and p-value. The remaining two columns show the mean and the standard deviation.

### 5.1.2 Between-Trial Questionnaire

Only three participants from the *NoVRS* group did not suffer from discomfort and nausea. All participants (regardless of the group) suffered from dizziness. Six participants (3 from the *NoVRS* group and three from the *VRS* group) suffered from fatigue. Five participants suffered from headache (3 from the *VRS* group and two from the *NoVRS* group). Nine participants suffered from eyestrain (3 participants from the *VRS* and 6 participants from the *NoVRS* group). More information is located in the supplementary material. We performed statistical tests on the full scores of the between-trial questionnaire and the scores of each symptom between the *VRS* group and the *NoVRS* group. Statistical differences were found in the discomfort and nausea scores. The *NoVRS* group had a lower discomfort score than the *VRS* group in blocks 3, 4, and 5. The Nausea score of the *VRS* was also significantly greater than that of the *NoVRS* group in block 5 of the experiment.

A summary of the descriptive statistics appears in Table 1. Figure 4 shows the discomfort and nausea scores. We only included these figures because they are the only measurements with significant statistical differences and where there is a visible difference between both groups. We included the rest of the figures for the rest of the symptoms in our additional material.

## 5.2 Biomechanical Results

Figure 5 shows the comparisons of biomechanical measurements between the two groups. Statistical differences were found on CoM in blocks 2 and 6 (see Table 1, last two rows). At both blocks, the *VRS* group showed a greater CoM displacement than the *NoVRS* group. No statistically significant differences were found in any of the other biomechanical measures.

## 5.3 EEG results

Figures 6, 8, 9, and 10 show the group ERSP results at the Fz, Cz, Pz and T8 channels respectively. Each figure contains the following information: the top rows show the ERSP of the *VRS* group. The

Measure	B	Stat, p-val	$\mu$	$\sigma$
CoM	2	$\chi^2(14) = 4.41, 0.03$	VRS 0.31 NoVRS 0.22	0.11 0.08
CoM	6	$\chi^2(11) = 4.2, 0.04$	VRS 0.33 NoVRS 0.25	0.07 0.06

Table 2: Biomechanical measurements with significant differences. CoM stands for Center of Mass. The second column is the block number. The third column shows the statistic and p-value. The remaining two columns show the mean and the standard deviation.

middle rows show the ERSP of the *NoVRS* group. Finally, the bottom rows show the statistical difference between the two groups after the permutation test.

In the rows showing ERSP labelled with *VRS* and *NoVRS*, the red color represents power increases, while blue represents power decreases. In the last row, the red color denotes that the *VRS* group has a statistically larger power than the *NoVRS*. The blue color denotes that the *VRS* group has statistically lower power. A summary of the increases and decreases at each frequency appears in Table 3, at the bottom row.

Figure 6 shows how the *VRS* group had a significantly lower Fz power at the delta frequencies at blocks 1 through 4. The *VRS* group had a significantly higher theta power at experiment blocks 1, 2 and 5. The alpha and beta frequencies were lower at experiment blocks 2 and 5, and the gamma frequencies were lower at experiment blocks 2, 3, 4, and 5.

Figure 8 shows a significant decrease in Cz delta power through the experiment. A decrease in theta power in blocks 2, 3, 4, 5, and 6. A low-alpha power decrease from the *VRS* group at experiment blocks 2, 3, 4, 5, and 6. A beta decrease at experiment blocks 5 and 6. And finally a significant decrease in the gamma power at experiment block 5.

Figure 9 shows a significant decrease in Pz delta power from the *VRS* group at experiment blocks 1 and 3. The *VRS* group also had significant theta decreases in experiment blocks 1, 3 and 6. Finally, there was a significant beta decrease in experiment block 2.

Finally, Figure 10 shows a strong decrease in T8 delta frequency from the *VRS* group throughout the experiment. There is also a significant decrease from the *VRS* group at the theta frequencies at experiment blocks 1 through 3. There is an alpha frequency decrease at experiment blocks 2 and 3. A beta frequency decrease at experiment block 2, and a decrease at the gamma frequency in experiment blocks 2 and 5.

## 6 DISCUSSION

### 6.1 Posture Instability Theory and EEG

No biomechanical measurements presented statistical differences but the difference in the Center of Mass. CoM showed differences within blocks 2 and 6. Block 2 has a corresponding TG level of 2x and was the first block when the participant experienced a perceivable disparity in body motion between real and virtual worlds. The result suggests that the *VRS* group initially had trouble adapting to the new perceivable TG level. Indeed, during the post-hoc interview, multiple users in the *VRS* group reported being surprised by the change in the TG level and commented that more time was needed to adapt to the sudden change in the virtual environment.

The statistically significant differences in the CoM appeared at Block 2, one experimental block before we found statistical differences in the BTQ. These findings confirm the primary assumption of the postural instability theory, which states that postural differences will appear before the onset of subjective symptoms [64]. Our EEG results in the central-theta frequency corroborate these findings. Different studies with VR HMD have reported these changes in participants that struggle to adjust posture or to maintain upright

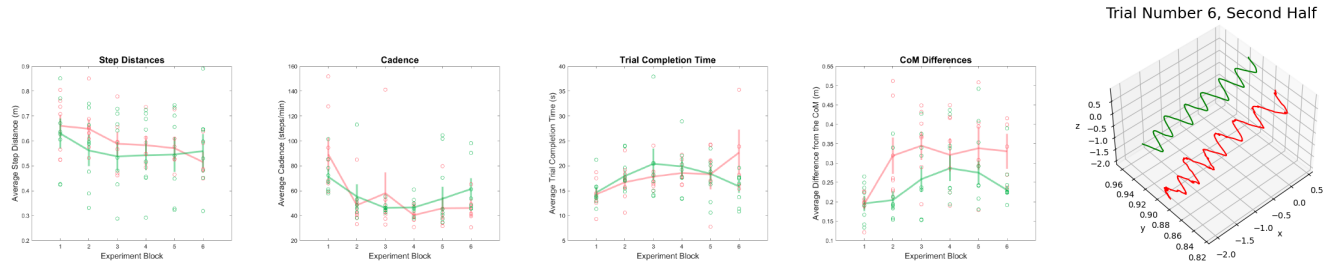


Figure 5: Biomechanical measurements of the *NoVRS* group (green) and the *VRS* group (red). From left to right: step distance, cadence, trial completion time, CoM differences, and an example 3D plot of CoM. We only show the second half of the trial to avoid visual clutter.

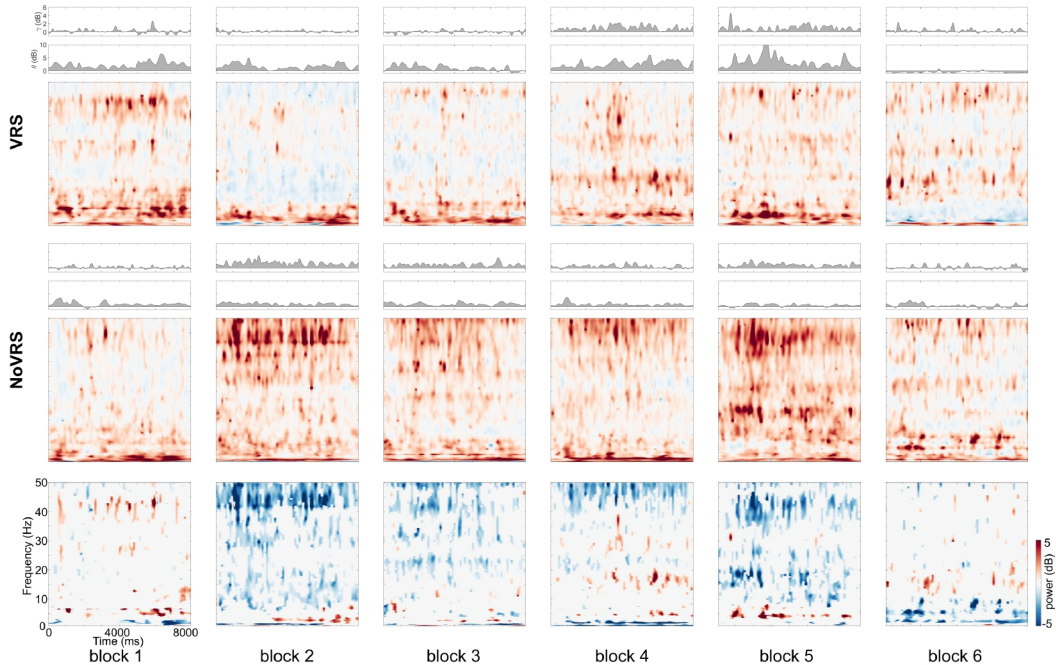


Figure 6: The Event-Related Spectral Dynamics (ERSD) of the **Fz** channel. The top subplot shows the ERSD of the *VRS* group, the middle shows the ERSD of the *NoVRS* group, and the bottom shows the statistical difference ( $p < 0.05$ ) between the *VRS* and *NoVRS* groups.

balance [14, 26, 69]. Given the relationship between the changes in posture and this signal, observation of the central-theta frequency can be used as an alternative method to identify if the participant is suffering from postural changes that lead to VR sickness.

Our EEG preliminary results yielded more important insights into the participants' cognitive performance. The EEG result suggests that *VRS* group did maintain postural control but at the cost of a higher mental effort. The *VRS* group has a significantly lower alpha power through blocks 2, 3, and 4. It has been well-established that alpha power (in the parietal brain region) was inversely correlated with mental workload [80]. The suppression of alpha power was also reported when the participant consciously adjusted their posture while standing [70, 84] and while walking [4]. Interestingly, when walking with a prosthesis, a similar reduction in alpha and gamma bands have been reported when the cognitive-motor task demands increased [61, 68]. In addition, the increased theta power in the frontal area of the *VRS* group also concurs with a series of works from Slobounov et al. [70–73] which found the theta power increased when the participant experienced postural sways. In sum, the lower alpha power (in frontal and parietal) and higher theta power (in frontal) of the *VRS* group seem to suggest that although *VRS* group could complete the tasks without significant changes in pos-

tural stability or gait parameters, they still found the task mentally challenging, which took more effort to complete them.

For the *NoVRS* group, their higher delta power also supports the argument that postural instability theory plays an important role in the mobile VR setup. The increased delta and theta powers were found when the participant was capable of engaging in cognitive-motor tasks, such as visual information processing and postural adjustment [20, 35]. Presacco et al. [60] also observed an increased delta power when the participants engaged in precision walking tasks. These findings suggest that the *NoVRS* group exhibited a better cognitive capability to continuously update their postural control strategy when compared to the *VRS* group.

In sum, despite both *VRS* and *NoVRS* groups having similar biomechanical measurements, the EEG data provides additional insights into the cognitive performance differences. The brain activities of *VRS* group exhibited similar patterns that were previously linked to higher cognitive workload and postural instability. In contrast, the *NoVRS* group showed brain activities that were expected when the participant is capable of performing complex motor tasks such as postural balance control and fine walking movements.

## 6.2 Future VR Headset Design

Table 3 shows a list of works that used EEG to measure and understand VR sickness. Our experiment used a novel experimental protocol in a mobile VR setup and resulted in some contradictory EEG results from some previous works. As discussed in the previous section, the difference might be attributed to the cognitive activities related to postural control. In contrast, the EEG difference in previous works might represent the brain activities related to the sensory conflict. Nevertheless, most works, including ours, seem to agree that the fluctuation of low-frequency power along the frontal and parietal midline correlates with VR sickness.

This finding suggests that the ideal locations for an EEG add-on for VR sickness detection on a VR headset might be at the frontal and parietal midline region. Because the changes in the low frequency seem to be a common phenomenon in most VR sickness experiments, it might be possible to train a single classifier that can be generalised to different virtual environments and VR setups (stationary or walking).

The result also suggests that postural instability theory is worth further investigation as most consumer VR headsets allow natural walking in the virtual environment. In addition, the biomechanical measurements alone might not be able to capture the full picture of the postural instability theory. Additional measurements such as EEG or other biosignals might be necessary for the future investigation alone this direction.

## 7 LIMITATIONS AND FUTURE WORK

One of the main limitations of this study is the number of participants. Due to the pandemic constraint, IRB in our university does not allow prolonged contact with participants. As a result, we could only recruit 21 participants for the experiment. More participants will strengthen the result and reduce the risk of having a biased group.

Previous VR sickness works have suggested that participants experiencing VR sickness also reported higher task load [6]. Recent works also found that the task workload might also affect VR sickness [67]. One of our EEG-based findings is that the participant with VR sickness could maintain postural stability at the cost of a higher mental workload. We did not use the NASA-TLX task load questionnaire at the end of the experiment because we originally considered the walking task simple enough for all participants. Retrospectively, we believe a between-trial workload questionnaire might provides additional supports our EEG findings. However, the questionnaire might not be able to distinguish whether the workload is because of VR sickness or the effort to maintain postural control.

In this experiment, we split the participant into two groups based on the SSQ questionnaire score, similar to previous EEG experiments [29, 41]. However, as mentioned in the recent work by Hirzle et al. [22], many important factors related to VR sickness, such as digital eye strain and ergonomics, are largely ignored by SSQ. In particular, the ergonomic symptoms, such as anxiety about the headset's weight and how the headset affects the movement, are relevant to the postural instability theory. It would be interesting to group participants based on the more comprehensive VR sickness questionnaire and re-examine the result.

Our work contains several limitations in the area of data analysis. The current analysis of CoM focused on the spatial dynamics of postural instability. We envision studying the temporal dynamics of the CoM of participants to provide a superior analysis on the status of the CoM and its relationship with the EEG signals.

A temporal analysis of the EEG results can shed some more information of the nature of our results. Our results are applicable considering that the level of VR sickness will be gradually incremented, which only applies to a certain number of VR applications. A comparative analysis within group between each of the experiment blocks can help us understand more about the additive effects of VR sickness. Furthermore, another experiment randomizing the levels

of TG can help understand the differences between additive effects vs spontaneous changes of TG.

The current work analyzed the EEG data using a channel-based approach and reported the EEG result along the midline. The 64-channel EEG signals are mainly used for noise removal in the pre-processing stage. With 64-channel EEG data, it might also be possible to localize the electrical activity in the brain using approaches such as sLORETA [57]. We have made some initial attempts in this direction, but the mobile VR setup and potentially the VR sickness symptoms significantly affect the quality of the results. Further investigation is needed to localize the distributed cortical sources of EEG activity.

## 8 CONCLUSION

This paper presents the first EEG-based study on VR sickness when the user actively walks in a virtual environment while wearing a VR headset. A comprehensive list of EEG-based studies on VR sickness was presented in the paper for guiding the future research. Our study used multiple measurements, including full-body motion capture and EEG. Our EEG results together with the results in the difference of Center of Mass suggests that the VRS group spent higher cognitive efforts to maintain the postural balance during the experiment. The result suggests that the postural instability theory might play an important role in understanding VR sickness in mobile VR setups.

## ACKNOWLEDGMENTS

This work was supported in part by the Australian Research Council (ARC) under discovery grant DP210101093 and DP220100803, and the UTS Human-Centric AI Centre funding sponsored by GrapheneX (2023-2031). Research was also sponsored in part by the Australia Defence Innovation Hub under Contract No. P18-650825, Australian Cooperative Research Centres Projects (CRC-P) Round 11 CRCPXI000007, US Office of Naval Research Global under Cooperative Agreement Number ONRG - NICOP - N62909-19-1-2058, and AFOSR – DST Australian Autonomy Initiative agreement ID10134. We also thank the NSW Defence Innovation Network and NSW State Government of Australia for financial support in part of this research through grant DINPP2019 S1-03/09 and PP21-22.03.02. We would also like to thank Mr. Mario Flores for the support recording and editing our multimedia content.

## REFERENCES

- [1] R. Abiri, S. Borhani, E. W. Sellers, Y. Jiang, and X. Zhao. A comprehensive review of eeg-based brain–computer interface paradigms. *Journal of neural engineering*, 16(1):011001, 2019.
- [2] K. Adistambha, C. H. Ritz, and I. S. Burnett. Motion classification using dynamic time warping. In *Proceedings of the 2008 IEEE 10th Workshop on Multimedia Signal Processing, MMSP 2008*, pp. 622–627, 2008. doi: 10.1109/MMSP.2008.4665151
- [3] T. Alsop. Virtual Reality (VR) - statistics & facts, 2021.
- [4] R. Beurskens, F. Steinberg, F. Antoniewicz, W. Wolff, and U. Granacher. Neural Correlates of Dual-Task Walking: Effects of Cognitive versus Motor Interference in Young Adults. *Neural Plasticity*, 2016, 2016. doi: 10.1155/2016/8032180
- [5] C.-J. Chang, T.-F. Yang, S.-W. Yang, and J.-S. Chern. Cortical modulation of motor control biofeedback among the elderly with high fall risk during a posture perturbation task with augmented reality. *Front. Aging Neurosci.*, 8:80, Apr. 2016.
- [6] E. Chang, H. T. Kim, and B. Yoo. Virtual reality sickness: A review of causes and measurements. *International Journal of Human–Computer Interaction*, 36(17):1658–1682, 2020. doi: 10.1080/10447318.2020.1778351
- [7] W. E. Chelen, M. Kabrisky, and S. K. Rogers. Spectral analysis of the electroencephalographic response to motion sickness. *Aviat. Space Environ. Med.*, 64(1):24–29, Jan. 1993.
- [8] Y.-C. Chen, J.-R. Duann, S.-W. Chuang, C.-T. C.-L. Lin, L.-W. Ko, T.-P. Jung, and C.-T. C.-L. Lin. Spatial and temporal EEG dynamics

Paper	Frontal	Central	Parietal	Occipital	Temporal	Protocol	Experiment	Apparatus	EEG
Chelen 1993 [7]	$\delta \uparrow \theta \uparrow$				$\delta \uparrow \theta \uparrow$	Passive	Coriolis stimulation	Coriolis stimulation	14-ch
Min 2004 [49]	$\theta \downarrow$	$\theta \downarrow$				Passive	Virtual driving video	2D display	2-ch (Fz Cz)
Li 2020 [40]**						Passive	Virtual navigation video	2D display	8-ch
Lim 2021 [41]	$\delta \uparrow \theta \uparrow \alpha \downarrow$	$\delta \uparrow \theta \uparrow \alpha \downarrow$				Passive	Virtual fly video	2D display	256-ch
Jang 2022 [29]	$\delta \uparrow \alpha \downarrow$		$\delta \uparrow \alpha \downarrow$	$\delta \uparrow \alpha \downarrow$	$\delta \uparrow \alpha \downarrow$	Passive	Virtual fly video	2D display	256-ch
Naqvi 2015 [50]		$\theta \downarrow^*$				Passive	Virtual navigation video	2D and 3D displays	128-ch
Kim 2005 [34]	$\delta \uparrow \beta \downarrow$		$\beta \downarrow$		$\delta \uparrow \beta \downarrow$	Passive	Virtual navigation video	CAVE	9-ch
Park 2008 [56]	$\theta \downarrow$	$\theta \downarrow$				Passive	Virtual navigation video	CAVE	2-ch (Fz Cz)
Lin 2007 [42]	$\alpha \uparrow \beta \uparrow$		$\alpha \uparrow \beta \uparrow$			Passive	Autopilot on a winding road	CAVE + 6 DoF driving simulator	32-ch
Chen 2010 [8]	$\alpha \downarrow$		$\alpha \downarrow$	$\delta \uparrow \theta \uparrow$		Passive	Autopilot on a winding road	CAVE + 6 DoF driving simulator	32-ch
Chuang 2016 [9]	$\alpha \uparrow \gamma \uparrow$		$\alpha \uparrow \gamma \uparrow$	$\alpha \uparrow \gamma \uparrow$		Passive	Autopilot on a winding road	CAVE + 6 DoF driving simulator	32-ch
Huang 2021 [25]	$\alpha \uparrow$		$\alpha \uparrow$	$\alpha \uparrow$		Passive & Active	A driver actively drive on a winding road with a passenger	CAVE + 6 DoF driving simulator	64-ch x 2
Recenti 2021 [63]		$\beta \downarrow^*$				Passive	Simulation of standing on a floating small boat	HMD + moving platform	64-ch (dry)
Kim 2019 [33]				$\alpha \uparrow$		Passive	Videos of roller coaster ride diving driving airplane control	HMD	62-ch
Wu 2020 [85]**	$N2 \uparrow P3 \downarrow$	$N2 \uparrow P3 \downarrow$	$N2 \uparrow P3 \downarrow$			Passive	Virtual navigation video	HMD	24-ch
Nurnberger 2021 [53]		$\delta \uparrow \theta \uparrow \alpha \uparrow$	$\delta \uparrow \theta \uparrow \alpha \uparrow$	$\delta \uparrow \theta \uparrow \alpha \uparrow$	$\delta \uparrow \theta \uparrow \alpha \uparrow$	Passive	Virtual fly controlled by an observer	HMD	18-ch
Krokos 2022 [36]		$\delta \uparrow \theta \uparrow \alpha \uparrow$				Passive	Virtual fly video	HMD	14-ch (dry)
<b>Ours</b>	$\delta \downarrow \theta \uparrow \alpha \downarrow$ $\beta \downarrow \gamma \downarrow$	$\delta \downarrow \theta \downarrow \alpha \downarrow$ $\beta \downarrow$	$\delta \downarrow \theta \downarrow \alpha \downarrow$ $\beta \downarrow$		$\delta \downarrow \theta \downarrow \beta \downarrow$ $\gamma \downarrow$	Active	Virtual navigation with natural walking	HMD	64-ch

Table 3: Previous EEG-based works on motion sickness and VR sickness. The table is sorted according to the apparatus and experiment protocol used. All experiments except ours require the participants to stay in a sitting posture. All but one previous experiment [25] require the participants to perceive the pre-generated visual stimuli passively. \* [50, 63] report the average power changes across all chs.\*\* [40] did not report frequency band activities but only focused on the classification of the signal. [85] used the amplitude of event-related potential (ERP, N2 and P3) as the indicators for VR sickness.

- of motion sickness. *NeuroImage*, 49(3):2862–2870, feb 2010. doi: 10.1016/J.NEUROIMAGE.2009.10.005
- [9] S. W. Chuang, C. H. Chuang, Y. H. Yu, J. T. King, and C. T. Lin. EEG Alpha and Gamma Modulators Mediate Motion Sickness-Related Spectral Responses. *International Journal of Neural Systems*, 26(2):1650007, mar 2016. doi: 10.1142/S0129065716500076
- [10] M. Cohen. *Analyzing Neural Time Series Data*. MIT Press, Massachusetts, 2014.
- [11] A. Delorme and S. Makeig. EEGLAB: an open source toolbox for analysis of single-trial EEG dynamics including independent component analysis. *Journal of Neuroscience Methods*, 134(1):9–21, mar 2004. doi: 10.1016/J.JNEUMETH.2003.10.009
- [12] A. Delorme, T. Mullen, C. Kothe, Z. Akalin Acar, N. Bigdely-Shamlo, A. Vankov, and S. Makeig. EEGLAB, SIFT, NFT, BCILAB, and ERICA: New Tools for Advanced EEG Processing. *Computational Intelligence and Neuroscience*, 2011:1–12, 2011. doi: 10.1155/2011/130714
- [13] T. T. N. Do, C. T. Lin, and K. Gramann. Human brain dynamics in active spatial navigation. *Scientific Reports*, 11(1):1–12, jun 2021. doi: 10.1038/s41598-021-92246-4
- [14] A. E. Edwards, O. Guven, M. D. Furman, Q. Arshad, and A. M. Bronstein. Electroencephalographic Correlates of Continuous Postural Tasks of Increasing Difficulty. *Neuroscience*, 395:35–48, 2018. doi: 10.1016/j.neuroscience.2018.10.040
- [15] B. V. Ehinger, P. Fischer, A. L. Gert, L. Kaufhold, F. Weber, G. Pipa, and P. König. Kinesthetic and vestibular information modulate alpha activity during spatial navigation: A mobile eeg study. *Frontiers in Human Neuroscience*, 8:71, 2 2014. doi: 10.3389/FNHN.2014.00071/ABSTRACT
- [16] T. Feigl, D. Roth, S. Gradl, M. Wirth, M. E. Latoschik, B. M. Eskofier, M. Philippse, and C. Mutschler. Sick Moves! Motion Parameters as Indicators of Simulator Sickness. *IEEE Transactions on Visualization and Computer Graphics*, 25(11):3146–3157, nov 2019. doi: 10.1109/TVCG.2019.2932224
- [17] B. T. Files, V. J. Lawhern, A. J. Ries, and A. R. Marathe. A Permutation Test for Unbalanced Paired Comparisons of Global Field Power. *Brain Topography*, 29(3):345–357, may 2016. doi: 10.1007/S10548-016-0477-3/FIGURES/5
- [18] J. Frey, M. Daniel, J. Castet, M. Hachet, and F. Lotte. Framework for electroencephalography-based evaluation of user experience. In *Proceedings of the 2016 CHI Conference on Human Factors in Computing Systems*, pp. 2283–2294, 2016.
- [19] T. Grechkin, J. Thomas, M. Azmandian, M. Bolas, and E. Suma. Revisiting detection thresholds for redirected walking: Combining translation and curvature gains. In *Proceedings of the ACM Symposium on Applied Perception*, pp. 113–120, 2016.
- [20] T. Harada, I. Miyai, M. Suzuki, and K. Kubota. Gait capacity affects cortical activation patterns related to speed control in the elderly. *Experimental Brain Research*, 193(3):445–454, 2009. doi: 10.1007/s00221-008-1643-y
- [21] M. Hayashi, K. Okuyama, N. Mizuguchi, R. Hirose, T. Okamoto, M. Kawakami, and J. Ushiba. Spatially bivariate EEG-neurofeedback can manipulate interhemispheric inhibition. *eLife*, 11, jul 2022. doi: 10.7554/elife.76411
- [22] T. Hirzle, M. Cordts, E. Rukzio, J. Gugenheimer, and A. Bulling. A critical assessment of the use of SSQ as a measure of general discomfort in VR Head-Mounted displays. In *Proceedings of the 2021 CHI Conference on Human Factors in Computing Systems*, number Article 530 in CHI ’21, pp. 1–14. Association for Computing Machinery, New York, NY, USA, May 2021.
- [23] C. G. Horlings, M. G. Carpenter, U. M. Küng, F. Honeygger, B. Wiederhold, and J. H. Allum. Influence of virtual reality on postural stability during movements of quiet stance. *Neuroscience Letters*, 451(3):227–231, feb 2009. doi: 10.1016/j.neulet.2008.12.057
- [24] A. Hreljac and R. N. Marshall. Algorithms to determine event timing during normal walking using kinematic data. *Journal of Biomechanics*, 33(6):783–786, jun 2000. doi: 10.1016/S0021-9290(00)00014-2
- [25] K.-C. Huang, A. R. John, T.-P. Jung, W.-F. Tsai, Y.-H. Yu, and C.-T. Lin. Comparing the differences in brain activities and neural comodulations associated with motion sickness between drivers and passengers. *IEEE Trans. Neural Syst. Rehabil. Eng.*, 29:1259–1267, July 2021.
- [26] T. Hülsdünker, A. Mierau, C. Neeb, H. Kleinöder, and H. K. Strüder. Cortical processes associated with continuous balance control as revealed by EEG spectral power. *Neuroscience Letters*, 592:1–5, 2015. doi: 10.1016/j.neulet.2015.02.049
- [27] V. Interrante, B. Ries, and L. Anderson. Seven league boots: A new metaphor for augmented locomotion through moderately large scale immersive virtual environments. In *2007 IEEE Symposium on 3D User Interfaces*, Mar. 2007.
- [28] O. Janeh, G. Bruder, F. Steinicke, A. Gulberti, and M. Poetter-Nerger. Analyses of Gait Parameters of Younger & Older Adults during (Non-)Isometric Virtual Walking. *IEEE Transactions on Visualization and Computer Graphics*, 24(10):2663–2674, 2017. doi: 10.1109/TVCG.2017.2771520
- [29] K.-M. Jang, M. Kwon, S. G. Nam, D. Kim, and H. K. Lim. Estimating objective (EEG) and subjective (SSQ) cybersickness in people with susceptibility to motion sickness. *Appl. Ergon.*, 102:103731, July 2022.
- [30] A. Jasper, N. Cone, C. Meusel, M. Curtis, M. C. Dorneich, and S. B. Gilbert. Visually Induced Motion Sickness Susceptibility and Recovery Based on Four Mitigation Techniques. *Frontiers in Virtual Reality*, 1:582108, oct 2020. doi: 10.3389/fvrir.2020.582108
- [31] R. S. Kennedy, N. E. Lane, K. S. Berbaum, and M. G. Lilienthal. Simulator sickness questionnaire: An enhanced method for quantifying simulator sickness. *The International Journal of Aviation Psychology*, 3(3):203–220, 1993. doi: 10.1207/s15327108ijap0303\_3
- [32] H. K. Kim, J. Park, Y. Choi, and M. Choe. Virtual reality sickness questionnaire (VRSQ): Motion sickness measurement index in a virtual reality environment. *Appl. Ergon.*, 69:66–73, May 2018.
- [33] J.-Y. Kim, J.-B. Son, H.-S. Leem, and S.-H. Lee. Psychophysiological Alteration After Virtual Reality Experiences Using Smartphone-Assisted Head Mount Displays: An EEG-Based Source Localization Study. *Applied Sciences*, 9(12):2501, jun 2019. doi: 10.3390/app9122501
- [34] Y. Y. Kim, H. J. Kim, E. N. Kim, H. D. Ko, and H. T. Kim. Characteristic changes in the physiological components of cybersickness. *Psychophysiology*, 42(5):616–625, 2005. doi: 10.1007/s00234-005-1388-2
- [35] J. E. Kline, K. Poggensee, and D. P. Ferris. Your brain on speed: cognitive performance of a spatial working memory task is not affected by walking speed. *Frontiers in Human Neuroscience*, 8:288, 2014. doi: 10.3389/fnhum.2014.00288
- [36] E. Krokos and A. Varshney. Quantifying VR cybersickness using EEG. *Virtual Real.*, 26(1):77–89, Mar. 2022.
- [37] L. Kruse, E. Langbehn, and F. Stelncke. I Can See on My Feet while Walking: Sensitivity to Translation Gains with Visible Feet. In *25th IEEE Conference on Virtual Reality and 3D User Interfaces, VR 2018 - Proceedings*, pp. 305–312. Institute of Electrical and Electronics Engineers Inc., aug 2018. doi: 10.1109/VR.2018.8446216
- [38] D. Lafond, M. Duarte, and F. Prince. Comparison of three methods to estimate the center of mass during balance assessment. *Journal of Biomechanics*, 37(9):1421–1426, sep 2004. doi: 10.1016/S0021-9290(03)00251-3
- [39] J. J. LaViola. A discussion of cybersickness in virtual environments. *ACM SIGCHI Bulletin*, 32(1):47–56, jan 2000. doi: 10.1145/333329.333344
- [40] X. Li, C. Zhu, C. Xu, J. Zhu, Y. Li, and S. Wu. VR motion sickness recognition by using EEG rhythm energy ratio6 based on wavelet packet transform. *Computer Methods and Programs in Biomedicine*, 188:105266, 2020. doi: 10.1016/j.cmpb.2019.105266
- [41] H. K. Lim, K. Ji, Y. S. Woo, D. uk Han, D. H. Lee, S. G. Nam, and K. M. Jang. Test-retest reliability of the virtual reality sickness evaluation using electroencephalography (EEG). *Neuroscience Letters*, 743:135589, jan 2021. doi: 10.1016/j.neulet.2020.135589
- [42] C.-T. Lin, S.-W. Chuang, Y.-C. Chen, L.-W. Ko, S.-F. Liang, and T.-P. Jung. EEG effects of motion sickness induced in a dynamic virtual reality environment. *Conf. Proc. IEEE Eng. Med. Biol. Soc.*, 2007:3872–3875, 2007.
- [43] C. T. Lin, S. F. Tsai, and L. W. Ko. EEG-based learning system for online motion sickness level estimation in a dynamic vehicle environment. *IEEE Transactions on Neural Networks and Learning Systems*,

- 24(10):1689–1700, 2013. doi: 10.1109/TNNLS.2013.2275003
- [44] J. Liu, A. K. Singh, and C.-T. Lin. Using virtual global landmark to improve incidental spatial learning. *Scientific Reports*, 12(1):6744, 2022. doi: 10.1038/s41598-022-10855-z
- [45] J. Liu, A. K. Singh, A. Wunderlich, K. Gramann, and C. T. Lin. Redesigning navigational aids using virtual global landmarks to improve spatial knowledge retrieval. *npj Science of Learning* 2022 7:1, 7:1–12, 7 2022. doi: 10.1038/s41539-022-00132-z
- [46] S. Makeig, K. Gramann, T.-P. Jung, T. J. Sejnowski, and H. Poizner. Linking brain, mind and behavior. *Int. J. Psychophysiol.*, 73(2):95–100, Aug. 2009.
- [47] E. Maris and R. Oostenveld. Nonparametric statistical testing of EEG- and MEG-data. *Journal of Neuroscience Methods*, 164(1):177–190, aug 2007. doi: 10.1016/J.JNEUMETH.2007.03.024
- [48] N. McHugh, S. Jung, S. Hoermann, and R. W. Lindeman. Investigating a physical dial as a measurement tool for cybersickness in virtual reality. In *25th ACM Symposium on Virtual Reality Software and Technology*, pp. 1–5, 2019.
- [49] B.-C. Min, S.-C. Chung, Y.-K. Min, and K. Sakamoto. Psychophysiological evaluation of simulator sickness evoked by a graphic simulator. *Applied Ergonomics*, 35(6):549–556, nov 2004. doi: 10.1016/J.APERGO.2004.06.002
- [50] S. A. A. Naqvi, N. Badruddin, M. A. Jatoi, A. S. Malik, W. Hazabbah, and B. Abdullah. EEG based time and frequency dynamics analysis of visually induced motion sickness (VIMS). *Australas. Phys. Eng. Sci. Med.*, 38(4):721–729, Dec. 2015.
- [51] N. C. Nilsson, S. Serafin, and R. Nordahl. Establishing the range of perceptually natural visual walking speeds for virtual walking-in-place locomotion. *IEEE Transactions on Visualization and Computer Graphics*, 20(4):569–578, apr 2014. doi: 10.1109/TVCG.2014.21
- [52] N. C. Nilsson, S. Serafin, F. Steinicke, and R. Nordahl. Natural walking in virtual reality: A review, 2018. doi: 10.1145/3180658
- [53] M. Nürnberg, C. Klingner, O. W. Witte, and S. Brodoehl. Mismatch of Visual-Vestibular information in virtual reality: Is motion sickness part of the brains attempt to reduce the prediction error? *Front. Hum. Neurosci.*, 15:757735, Oct. 2021.
- [54] J. Palmer, K. Kreutz-Delgado, B. Rao, and S. Makeig. Modeling and estimation of dependent subspaces with non-radially symmetric and skewed densities. *Independent Component Analysis and Signal Separation*, 2007. doi: 10.1007/978-3-540-74494-8\_13
- [55] S. Palmisano, R. S. Allison, and J. Kim. Cybersickness in head-mounted displays is caused by differences in the user's virtual and physical head pose. *Frontiers in Virtual Reality*, 1:587698, 2020.
- [56] J.-R. Park, D.-W. Lim, S.-Y. Lee, H.-W. Lee, M.-H. Choi, and S.-C. Chung. Long-Term Study of Simulator Sickness: Differences in EEG Response Due to Individual Sensitivity. *International Journal of Neuroscience*, 118(6):857–865, jan 2008. doi: 10.1080/00207450701239459
- [57] R. D. Pascual-Marqui et al. Standardized low-resolution brain electromagnetic tomography (sloreta): technical details. *Methods Find Exp Clin Pharmacol*, 24(Suppl D):5–12, 2002.
- [58] E. M. M. Peck, B. F. Yuksel, A. Ottley, R. J. Jacob, and R. Chang. Using fnirs brain sensing to evaluate information visualization interfaces. In *Proceedings of the SIGCHI Conference on Human Factors in Computing Systems*, pp. 473–482, 2013.
- [59] S. M. Peterson, E. Rios, and D. P. Ferris. Transient visual perturbations boost short-term balance learning in virtual reality by modulating electrocortical activity. *Journal of Neurophysiology*, 120(4):1998–2010, 2018. doi: 10.1152/jn.00292.2018
- [60] A. Presacco, R. Goodman, L. Forrester, and J. L. Contreras-Vidal. Neural decoding of treadmill walking from noninvasive electroencephalographic signals. *Journal of Neurophysiology*, 106(4):1875–1887, 2011. doi: 10.1152/jn.00104.2011
- [61] A. L. Pruziner, E. P. Shaw, J. C. Rietschel, B. D. Hendershot, M. W. Miller, E. J. Wolf, B. D. Hatfield, C. L. Dearth, and R. J. Gentili. Biomechanical and neurocognitive performance outcomes of walking with transtibial limb loss while challenged by a concurrent task. *Experimental Brain Research*, 237(2):477–491, 2019.
- [62] L. Rebenitsch and C. Owen. Review on cybersickness in applications and visual displays. *Virtual Reality*, 20(2):101–125, 2016. doi: 10.1007/s10055-016-0285-9
- [63] M. Recenti, C. Ricciardi, R. Aubonnet, I. Picone, D. Jacob, H. Á. Svansson, S. Agnarsdóttir, G. H. Karlsson, V. Baeringsdóttir, H. Petersen, and P. Gargiulo. Toward Predicting Motion Sickness Using Virtual Reality and a Moving Platform Assessing Brain, Muscles, and Heart Signals. *Frontiers in Bioengineering and Biotechnology*, 9:132, apr 2021. doi: 10.3389/fbioe.2021.635661
- [64] G. E. Riccio and T. A. Stoffregen. An Ecological Theory of Motion Sickness and Postural Instability. *Ecological Psychology*, 1991. doi: 10.1207/s15326969eco0303\_2
- [65] M. T. Robert, L. Ballaz, and M. Lemay. The effect of viewing a virtual environment through a head-mounted display on balance. *Gait and Posture*, 48:261–266, jul 2016. doi: 10.1016/j.gaitpost.2016.06.010
- [66] D. Saredakis, A. Szpak, B. Birckhead, H. A. D. Keage, A. Rizzo, and T. Loetscher. Factors Associated With Virtual Reality Sickness in Head-Mounted Displays: A Systematic Review and Meta-Analysis. *Frontiers in Human Neuroscience*, 14:96, 2020. doi: 10.3389/fnhum.2020.00096
- [67] N. C. Sepich, A. Jasper, S. Fieffer, S. B. Gilbert, M. C. Dorneich, and J. W. Kelly. The impact of task workload on cybersickness. *Frontiers in Virtual Reality*, 3:943409, 2022.
- [68] E. P. Shaw, J. C. Rietschel, B. D. Hendershot, A. L. Pruziner, E. J. Wolf, C. L. Dearth, M. W. Miller, B. D. Hatfield, and R. J. Gentili. A comparison of mental workload in individuals with transtibial and transfemoral lower limb loss during dual-task walking under varying demand. *Journal of the International Neuropsychological Society*, 25(9):985–997, 2019.
- [69] A. R. Sipp, J. T. Gwin, S. Makeig, and D. P. Ferris. Loss of balance during balance beam walking elicits a multifocal theta band electrocorticital response. *Journal of Neurophysiology*, 110(9):2050–2060, 2013. doi: 10.1152/jn.00744.2012
- [70] S. Slobounov, M. Hallett, C. Cao, and K. Newell. Modulation of cortical activity as a result of voluntary postural sway direction: An EEG study. *Neuroscience Letters*, 442(3):309–313, sep 2008. doi: 10.1016/j.neulet.2008.07.021
- [71] S. Slobounov, M. Hallett, S. Stanhope, and H. Shibasaki. Role of cerebral cortex in human postural control: An EEG study. *Clinical Neurophysiology*, 116(2):315–323, feb 2005. doi: 10.1016/j.clinph.2004.09.007
- [72] S. M. Slobounov, W. Ray, B. Johnson, E. Slobounov, and K. M. Newell. Modulation of cortical activity in 2D versus 3D virtual reality environments: An EEG study. *International Journal of Psychophysiology*, 95(3):254–260, mar 2015. doi: 10.1016/j.ijpsycho.2014.11.003
- [73] S. M. Slobounov, E. Teel, and K. M. Newell. Modulation of cortical activity in response to visually induced postural perturbation: combined VR and EEG study. *Neuroscience letters*, 2013. doi: 10.1016/j.neulet.2013.05.001
- [74] K. Stanney, B. D. Lawson, B. Rokers, M. Dennison, C. Fidopiastis, T. Stoffregen, S. Weech, and J. M. Fulvio. Identifying Causes of and Solutions for Cybersickness in Immersive Technology: Reformulation of a Research and Development Agenda. *International Journal of Human-Computer Interaction*, 36(19):1783–1803, nov 2020. doi: 10.1080/10447318.2020.1828535
- [75] K. M. Stanney, R. S. Kennedy, and J. M. Drexler. Cybersickness is not simulator sickness. *Proceedings of the Human Factors and Ergonomics Society 41st Annual Meeting*, pp. 1138–1142, 1997. doi: 10.1177/107118139704100292
- [76] F. Steinicke, G. Bruder, J. Jerald, H. Frenz, and M. Lappe. Estimation of detection thresholds for redirected walking techniques. *IEEE transactions on visualization and computer graphics*, 16(1):17–27, 2009.
- [77] F. Steinicke, G. Bruder, J. Jerald, H. Frenz, and M. Lappe. Estimation of Detection Thresholds for Redirected Walking Techniques. *Ieee Tvcg*, 16(1):17–27, jan 2010. doi: 10.1109/TVCG.2009.62
- [78] W. B. Stone and III. *Psychometric Evaluation of the Simulator Sickness Questionnaire as a Measure of Cybersickness*. PhD thesis, Iowa State University, Ann Arbor, United States, 2017.
- [79] E. A. Suma, Z. Lipps, S. Finkelstein, D. M. Krum, and M. Bolas. Impossible spaces: Maximizing natural walking in virtual environments with self-overlapping architecture. *IEEE Transactions on Visualization and Computer Graphics*, 18(4):555–564, April 2012. doi: 10.

- [80] D. Tao, H. Tan, H. Wang, X. Zhang, X. Qu, and T. Zhang. A systematic review of physiological measures of mental workload. *International journal of environmental research and public health*, 16(15):2716, 2019.
- [81] C. A. Tirado Cortes, H.-T. Chen, and C.-T. Lin. Analysis of VR Sickness and Gait Parameters During Non-Isometric Virtual Walking with Large Translational Gain. In *The 17th International Conference on Virtual-Reality Continuum and Its Applications in Industry, VRCAI '19*. Association for Computing Machinery, New York, NY, USA, 2019. doi: 10.1145/3359997.3365694
- [82] S. Weech, S. Kenny, and M. Barnett-Cowan. Presence and Cybersickness in Virtual Reality Are Negatively Related: A Review. *Frontiers in Psychology*, 10:158, 2019.
- [83] G. Wilson, M. McGill, M. Jamieson, J. R. Williamson, and S. A. Brewster. Object Manipulation in Virtual Reality Under Increasing Levels of Translational Gain. *Proceedings of the 2018 CHI Conference on Human Factors in Computing Systems - CHI '18*, pp. 1–13, 2018. doi: 10.1145/3173574.3173673
- [84] E. Wittenberg, J. Thompson, C. S. Nam, and J. R. Franz. Neuroimaging of Human Balance Control: A Systematic Review. *Frontiers in Human Neuroscience*, 11:170, 2017. doi: 10.3389/fnhum.2017.00170
- [85] J. Wu, Q. Zhou, J. Li, X. Kong, and Y. Xiao. Inhibition-related N2 and p3: Indicators of visually induced motion sickness (VIMS). *Int. J. Ind. Ergon.*, 78:102981, July 2020.
- [86] C. Yildirim. Don't make me sick: investigating the incidence of cybersickness in commercial virtual reality headsets. *Virtual Reality*, 24(2):231–239, June 2020.
- [87] B. F. Yuksel, K. B. Oleson, L. Harrison, E. M. Peck, D. Afergan, R. Chang, and R. J. K. Jacob. Learn piano with BACh: An adaptive learning interface that adjusts task difficulty based on brain state. In *Proceedings of the 2016 CHI Conference on Human Factors in Computing Systems, CHI '16*, pp. 5372–5384. Association for Computing Machinery, New York, NY, USA, May 2016.
- [88] T. O. Zander and C. Kothe. Towards passive brain–computer interfaces: applying brain–computer interface technology to human–machine systems in general. *Journal of Neural Engineering*, 2011.

## A APPENDIX

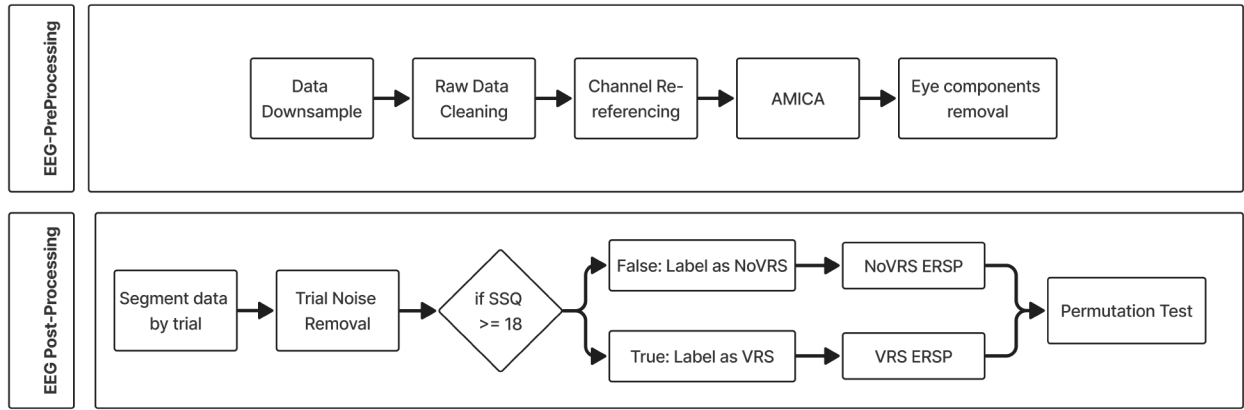


Figure 7: EEG processing pipeline summary.

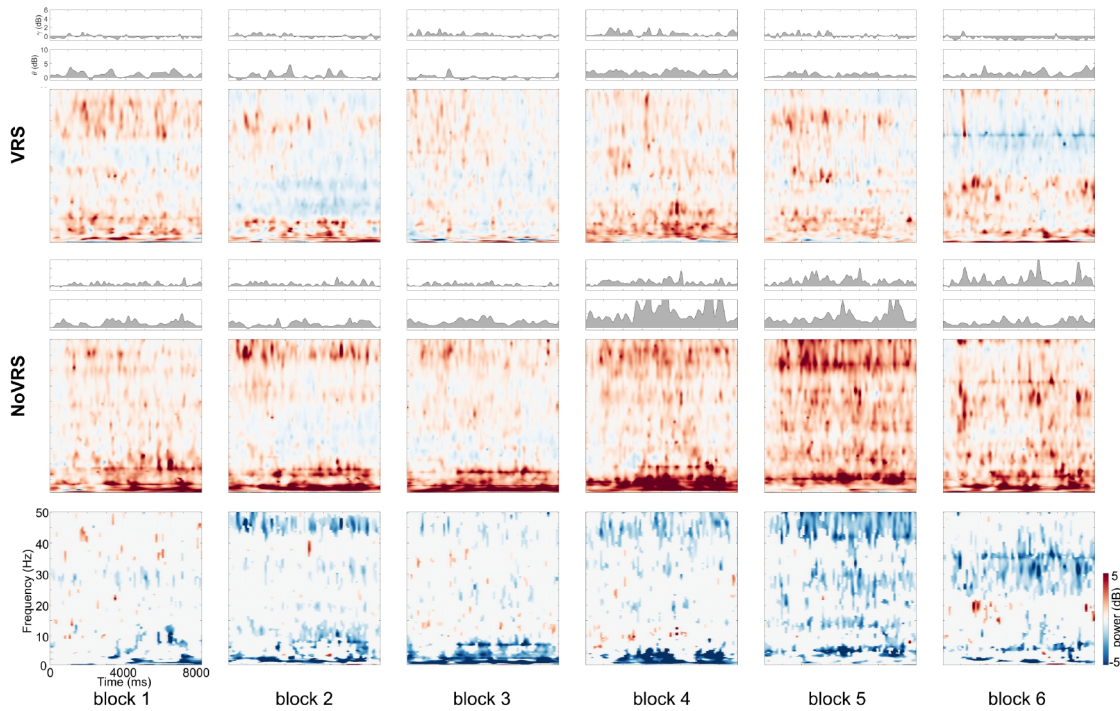


Figure 8: The Event-Related Spectral Dynamics (ERSP) of the **Cz** channel. The top subplot shows the ERSP of the *VRS* group, the middle shows the ERSP of the *NoVRS* group, and the bottom shows the statistical difference ( $p < 0.05$ ) between the *VRS* and *NoVRS* groups.

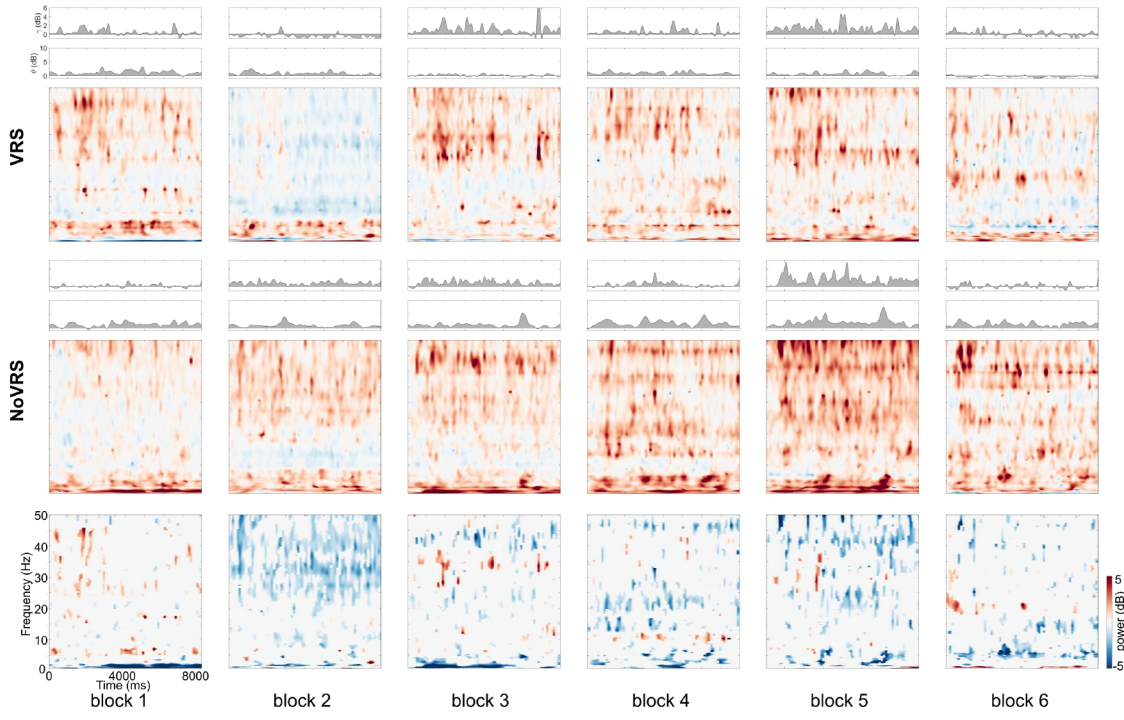


Figure 9: The Event-Related Spectral Dynamics (ERSP) of the **Pz** channel. The top subplot shows the ERSP of the *VRS* group, the middle shows the ERSP of the *NoVRS* group, and the bottom shows the statistical difference ( $p < 0.05$ ) between the *VRS* and *NoVRS* groups.

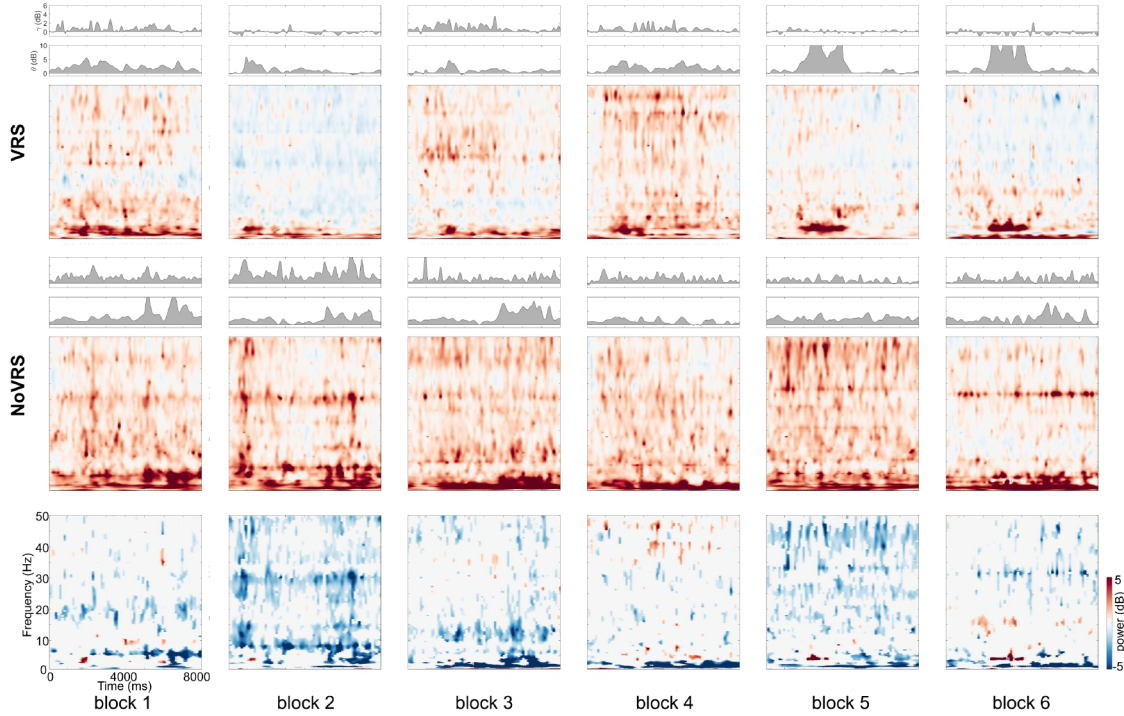


Figure 10: The Event-Related Spectral Dynamics (ERSP) of the **T8** channel. The top subplot shows the ERSP of the *VRS* group, the middle shows the ERSP of the *NoVRS* group, and the bottom shows the statistical difference ( $p < 0.05$ ) between the *VRS* and *NoVRS* groups.

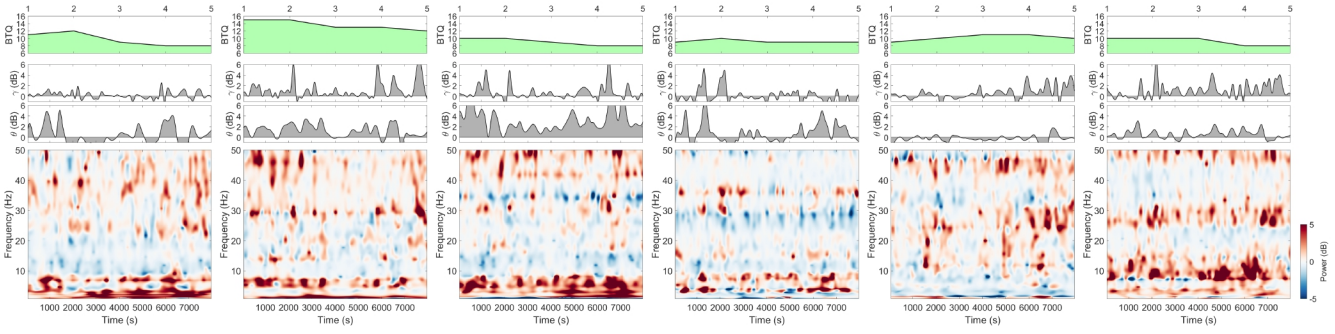


Figure 11: A representative VRS participant. The Event-Related Spectral Dynamics (ERSP) of the **Fz** channel from block 1 (first column) to block 6 (last column). The top subplot shows the value of the Between-Trial Questionnaire (BTQ), the middle shows the EEG power (dB) in the  $\gamma$  and  $\theta$  band, and the bottom shows the ERSP in the time-frequency domain.

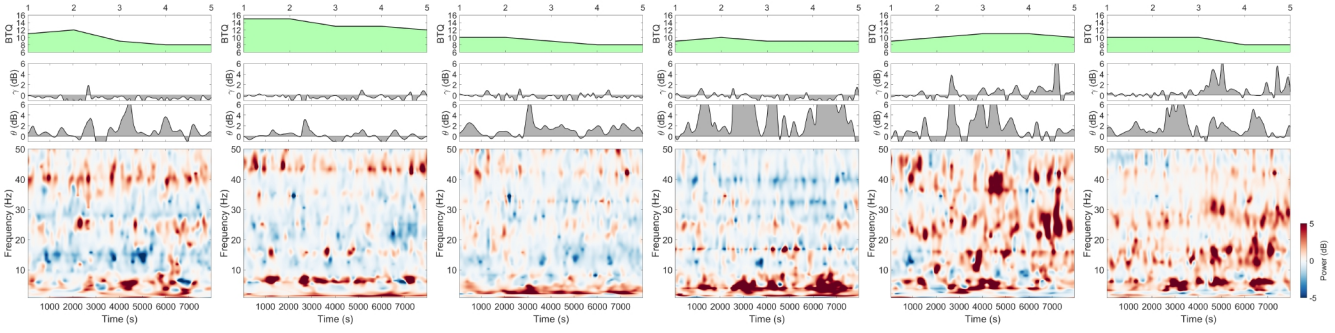


Figure 12: A representative VRS participant. The Event-Related Spectral Dynamics (ERSP) of the **Cz** channel from block 1 (first column) to block 6 (last column). The top subplot shows the value of the Between-Trial Questionnaire (BTQ), the middle shows the EEG power (dB) in the  $\gamma$  and  $\theta$  band, and the bottom shows the ERSP in the time-frequency domain.

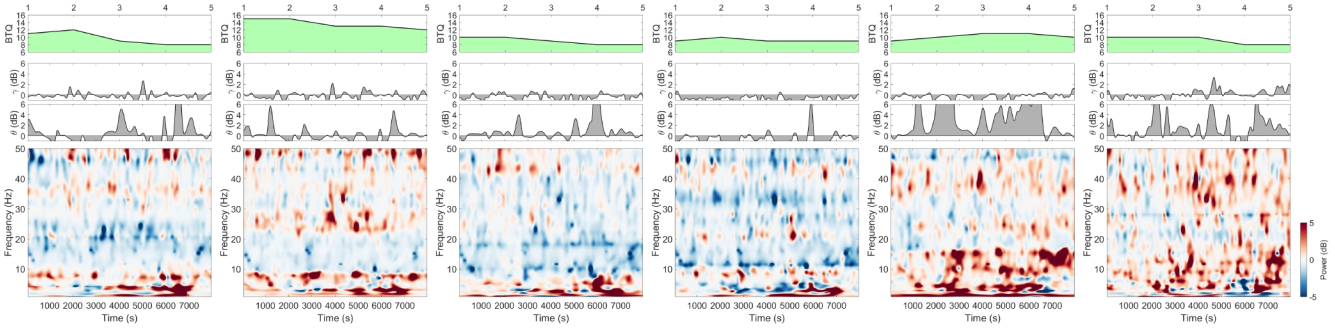


Figure 13: A representative VRS participant. The Event-Related Spectral Dynamics (ERSP) of the **Pz** channel from block 1 (first column) to block 6 (last column). The top subplot shows the value of the Between-Trial Questionnaire (BTQ), the middle shows the EEG power (dB) in the  $\gamma$  and  $\theta$  band, and the bottom shows the ERSP in the time-frequency domain.

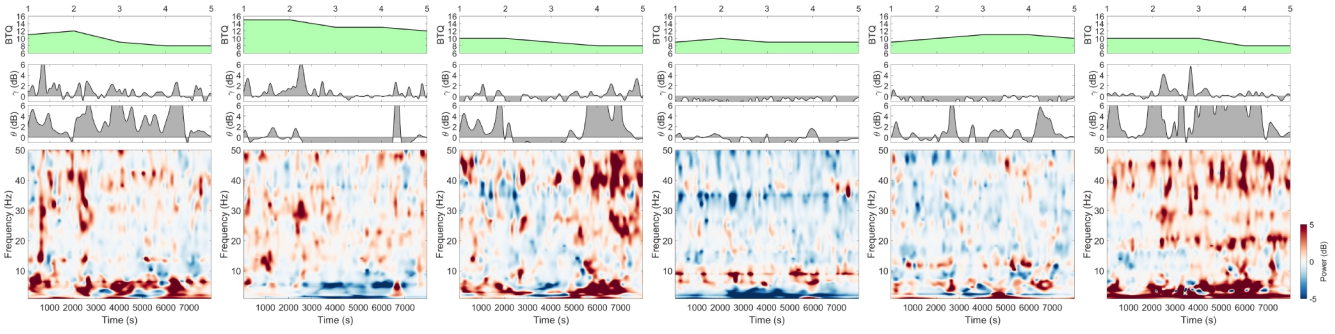


Figure 14: A representative *VRS* participant. The Event-Related Spectral Dynamics (ERSP) of the **T8** channel from block 1 (first column) to block 6 (last column). The top subplot shows the value of the Between-Trial Questionnaire (BTQ), the middle shows the EEG power (dB) in the  $\gamma$  and  $\theta$  band, and the bottom shows the ERSP in the time-frequency domain.

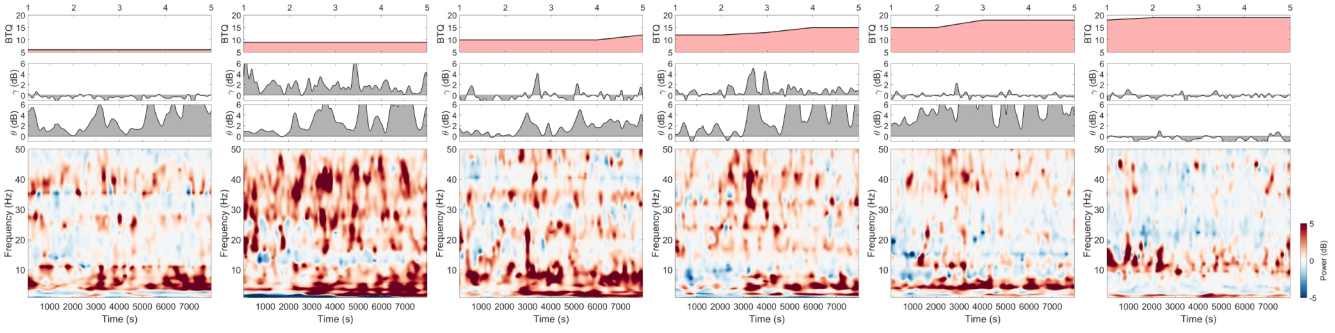


Figure 15: A representative *NoVRS* participant. The Event-Related Spectral Dynamics (ERSP) of the **Fz** channel from block 1 (first column) to block 6 (last column). The top subplot shows the value of the Between-Trial Questionnaire (BTQ), the middle shows the EEG power (dB) in the  $\gamma$  and  $\theta$  band, and the bottom shows the ERSP in the time-frequency domain.

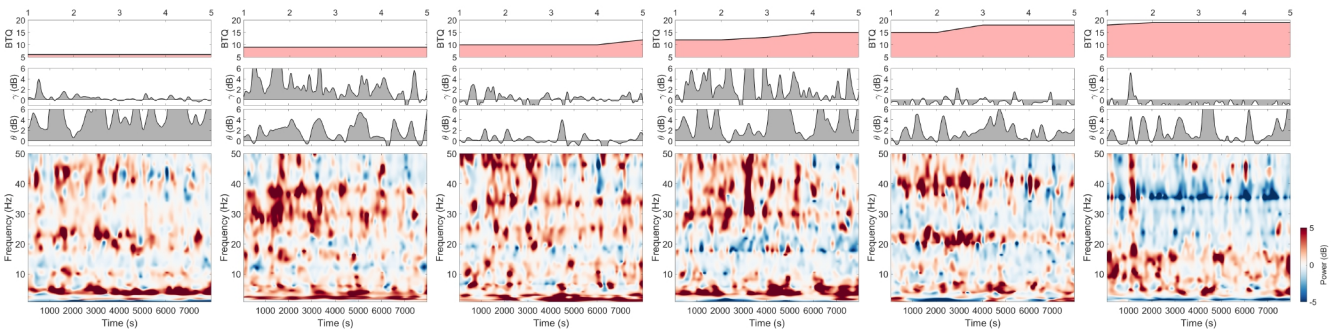


Figure 16: A representative *NoVRS* participant. The Event-Related Spectral Dynamics (ERSP) of the **Cz** channel from block 1 (first column) to block 6 (last column). The top subplot shows the value of the Between-Trial Questionnaire (BTQ), the middle shows the EEG power (dB) in the  $\gamma$  and  $\theta$  band, and the bottom shows the ERSP in the time-frequency domain.

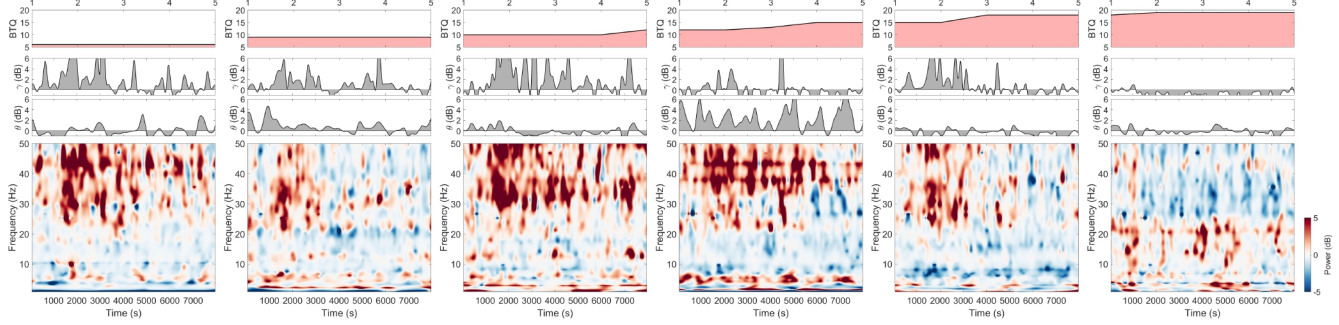


Figure 17: A representative *NovRS* participant. The Event-Related Spectral Dynamics (ERSD) of the **Pz** channel from block 1 (first column) to block 6 (last column). The top subplot shows the value of the Between-Trial Questionnaire (BTQ), the middle shows the EEG power (dB) in the  $\gamma$  and  $\theta$  band, and the bottom shows the ERSP in the time-frequency domain.

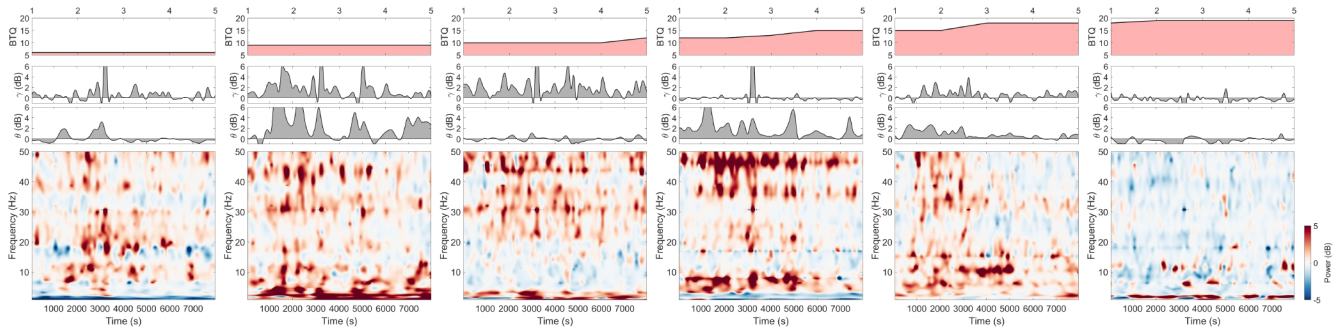


Figure 18: A representative *NovRS* participant. The Event-Related Spectral Dynamics (ERSD) of the **T8** channel from block 1 (first column) to block 6 (last column). The top subplot shows the value of the Between-Trial Questionnaire (BTQ), the middle shows the EEG power (dB) in the  $\gamma$  and  $\theta$  band, and the bottom shows the ERSP in the time-frequency domain.